

## Bright Side versus Dark Side of Star Formation — UV and IR Views

C.K. Xu and V. Buat

*IPAC, Caltech, 770 S. Welson Ave., Pasadena, CA91125, USA.*

*Laboratoire d'Astrophysique de Marseille, BP 8, Traverse du Siphon, 13376 Marseille Cedex 12, France.*



This is a review talk on the UV and infrared selected galaxies. The central question addressed is: do UV and infrared surveys see the 2 sides of star formation of the same population, or star formation of 2 different populations? We first review the literature on the UV and IR selected galaxy samples, try to quantify the difference and overlaps between these two populations of star forming galaxies. We then present some preliminary results of a GALEX/SWIRE comparison study for IR and UV selected galaxies at  $z=0.6$ , in an attempt to constrain the evolution of the dust attenuation and of stellar mass of these galaxies.

### 1 Introduction

The evolution of star forming galaxies tells much about the history of the universe. The star formation activity in these galaxies can be best studied by observing the emission from young massive stars in the rest frame UV and FIR. The UV observations record the direct light from the hot young stars, and the FIR observations collect star light absorbed and then re-emitted by the ubiquitous dust. A complete picture of star formation in the universe can only be obtained when the observations in these two wavebands are properly synthesized. Indeed, our knowledge on the star formation history of the universe ('Madau diagram') has been mostly derived from deep surveys in the rest frame UV and FIR. Many studies have been devoted to methods of deriving star formation rate of individual galaxies using the UV or FIR luminosities, particularly concerning the correction for the dust attenuation<sup>45 11 43 13 32 26</sup>. The strengths and shortcomings of these methods have been discussed thoroughly in the literature<sup>29 1 2 3 12 30 26</sup>. However, an arguably more important issue is the selection effect of the surveys that can be summed up by the following question: Do UV and IR surveys see the two sides ('dark' and 'bright') of the star formation of the same population of galaxies, or they see two different populations of star forming galaxies? This is important because if the correct answer is the latter, then even if one can estimate accurately the star formation rate for galaxies in surveys in one band, the

star formation in galaxies detected in the other band is still missing. Actually this question is in the core of an on-going debate on whether the SFR of  $z \sim 3$  universe can be derived from observations of Lyman-break galaxies (LBGs), which are UV selected star forming galaxies at  $z \sim 3$ <sup>1</sup>, given that SCUBA surveys in sub-millimeter (rest frame FIR for  $z \gtrsim 2$ ) detected many violent star forming galaxies at about the same redshift that are not seen by LBG surveys<sup>38 37</sup>.

This talk is arranged as follows: we'll first concentrate on local UV and IR selected galaxies and exam how much these two samples overlap. We compare their infrared to UV ratios, total luminosities, Hubble types, stellar mass, and the clustering behaviour. The comparison between the UV luminosity function for the IR selected galaxies and the GALEX UV luminosity function tells whether IR surveys miss a substantial population of UV galaxies. Similarly the infrared luminosity function for UV selected galaxies, when compared to IRAS luminosity function, tells what kind of IR galaxies are missed by the UV surveys. We'll exam in detail a population of IR-quiet UV galaxies, and compare luminous UV galaxies, the so called UVLGs that are recently discovered by GALEX, with ULIRGs. I'll then give a brief review on the literature of LBGs and SCUBA galaxies, focusing on their comparisons as UV and IR selected galaxies at redshift about 3. The last major topic is on UV and infrared galaxies at intermediate redshifts. Here I'll report early results of a GALEX/SWIRE comparison study on galaxies in the redshift range of 0.5 to 0.7, selected using photometric redshifts. We'll investigate evidence for evolution of the extinction in UV and IR selected galaxies, and for evolution of stellar mass in these galaxies. Then I'll wrap it up with a summary.

## 2 Local UV and IR Galaxies: How Much Do They Overlap?

Martin et al.<sup>31</sup> derived the infrared-UV bivariate luminosity function of local UV plus IR galaxies. There appears to be a saturation of UV luminosity at about  $2 \cdot 10^{10} L_{\odot}$ , beyond which the density drops fast. The distribution seems to be bi-modal, with galaxies of relatively low IR/UV ratios are reasonably well separated from those with high ratios. There is a strong dependence of the IR-to-UV ratio (the best indicator of the UV attenuation) on  $L_{tot}$ , which is the sum of the UV luminosity and infrared luminosity. Actually, the ratio increases almost proportionally with  $L_{tot}$ . The  $L_{tot}$  luminosity function of local UV plus IR galaxies has the form of log-normal. It appears that UV galaxies are absent in the high  $L_{tot}$  end ( $>$  a few  $10^{11} L_{\odot}$ ).

Buat et al.<sup>12</sup> compared the dust attenuation properties of NUV and FIR selected samples selected from GALEX and IRAS databases, respectively. The median value of the attenuation in NUV is found to be 1 mag for the NUV-selected sample, versus 2 mag for the FIR-selected one. Within both samples, the dust attenuation is found to correlate with the luminosity of the galaxies. These results are consistent with the pre-GALEX study of Iglesias-Páramo et al<sup>24</sup> using UV data of FOCA observations.

In order to exam the difference and overlaps between UV and IR selected galaxies quantitatively, we carried out detailed analysis in two local samples, one is Infrared selected and the other UV selected. These are the same samples discussed in Jorge Iglesias-Páramo's talk<sup>25</sup>, so I refer you to that paper for the details of the samples. Here I just mention the major selection criteria. The IR selected sample is taken from the PSCZ catalog, which are IRAS galaxies brighter than  $f_{60} = 0.6$  Jy and they all have measured redshifts. The UV sample is selected from galaxies brighter than NUV=17 magnitude found in the fields observed in the G1 stage of GALEX mission. In Fig.1 we show the IR-to-UV luminosity ratio distributions of UV and IR galaxies. They look rather different from each other. The overlap between the two distributions is only about 30%. The mean ratio of IR galaxies is one order of magnitude higher than that of the UV galaxies. The IR-to-UV ratio can be directly translated to the UV attenuation. As reported by Buat et al.<sup>12</sup>, the average UV attenuation of UV galaxies is only about 1 magnitude,

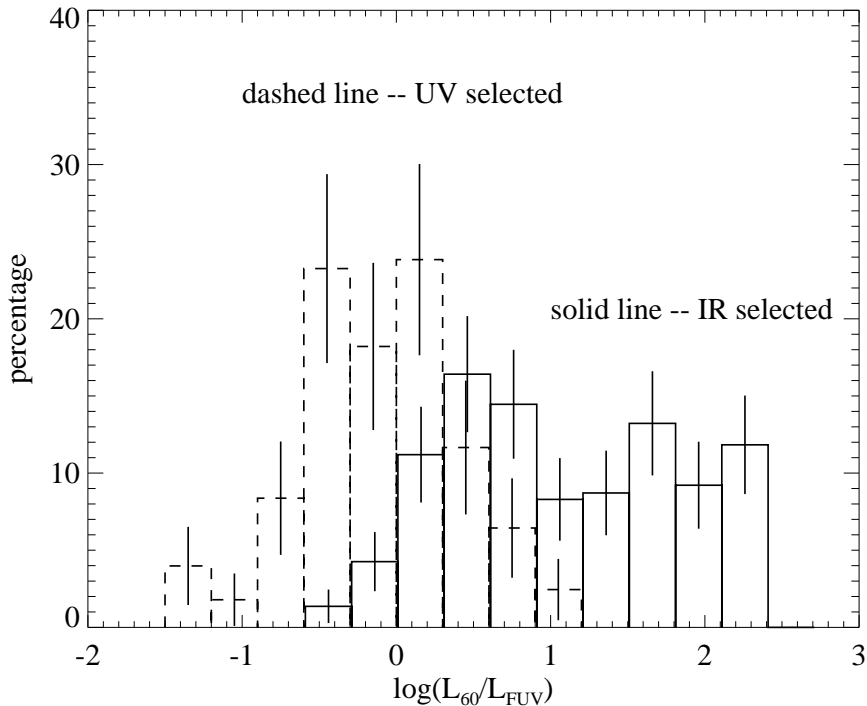


Figure 1: FIR/UV distributions of UV and IR galaxies.

while for IR selected galaxies, the average UV attenuation is above 2 magnitude.

Fig.2 shows the IR/UV ratio versus the  $L_{tot}$  for individual UV and IR galaxies. In this plot, the two populations are also separated, with the IR galaxies taking the high  $L_{tot}$ , high IR-to-UV ratio end of the correlation, and the UV galaxies occupying mostly the lower end of the correlation. This result can be explained by the strong correlation between the ratio and the  $L_{tot}$ , and the selection effect which biases the IR and UV samples toward the high and low ends of IR/UV ratios, respectively.

In Fig.3 we compare the Hubble type distributions of UV and IR galaxies. The overlap between the two distributions is  $\sim 60\%$ . There is a significant excess of Pec/Int/merg galaxies in the FIR selected sample (39%) compared to those in the UV selected sample (14%). For normal galaxies both UV and FIR selected samples peak in the bin of Sab/Sb/Sbc. Detailed analysis shows that the median type for normal UV galaxies is Sc and that of normal FIR galaxies is Sb.

Heinis et al. <sup>21</sup> carried out the angular correlation analysis for the UV population, using FOCA data. They found a correlation length of  $3.2 (+0.8, -2.3)$  Mpc  $(H_0/100)^{-1}$ . Compared to the correlation length of IRAS galaxies determined by Strauss et al. <sup>39</sup>, which is  $3.9 \pm 1.8$  Mpc  $(H_0/100)^{-1}$ , the UV galaxies seem to be slightly less clustered than IR galaxies, consistent with the fact that UV galaxies are preferentially later type spirals and irregulars.

Recent literature on galaxy formation and evolution has revealed the stellar mass as a fundamental variable in the characterization of galaxy populations <sup>7 27</sup>. And the K-band luminosity is the best estimator of the stellar mass <sup>4 5</sup>. Most of the galaxies in our UV and IR selected samples have been detected in K band by 2MASS. For a few sources that are not detected by 2MASS, we used the so called survival technique <sup>28 18 35</sup> to exploit the information content in the upper limits. The results are plotted in Fig.4. The solid histogram is the stellar mass distribution of IR galaxies and the dashed histogram is that of UV galaxies. The median K

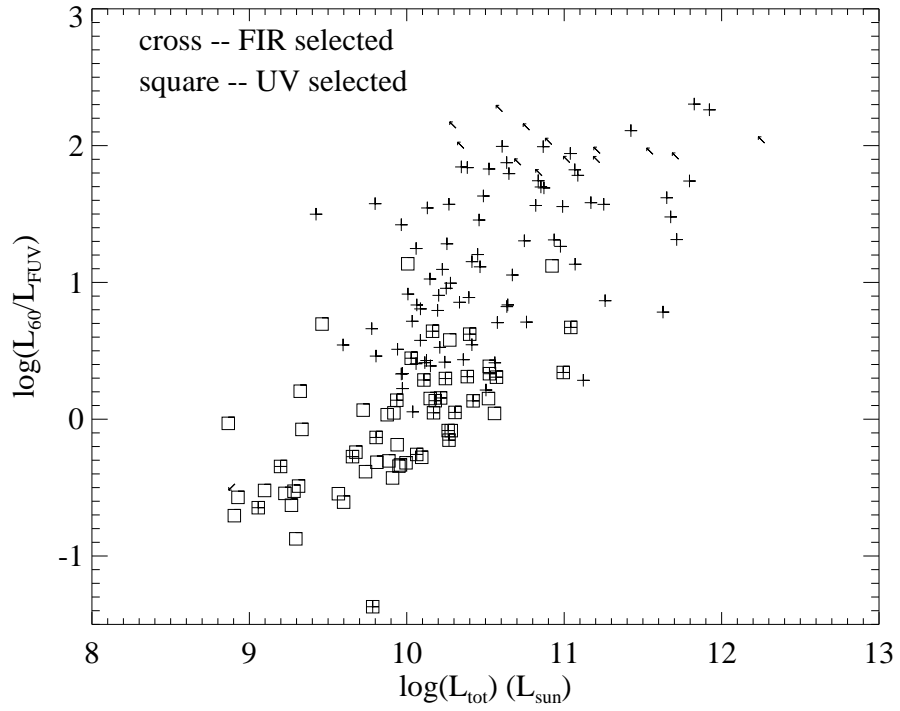


Figure 2: FIR/UV vs.  $L_{\text{tot}}$  of individual galaxies.

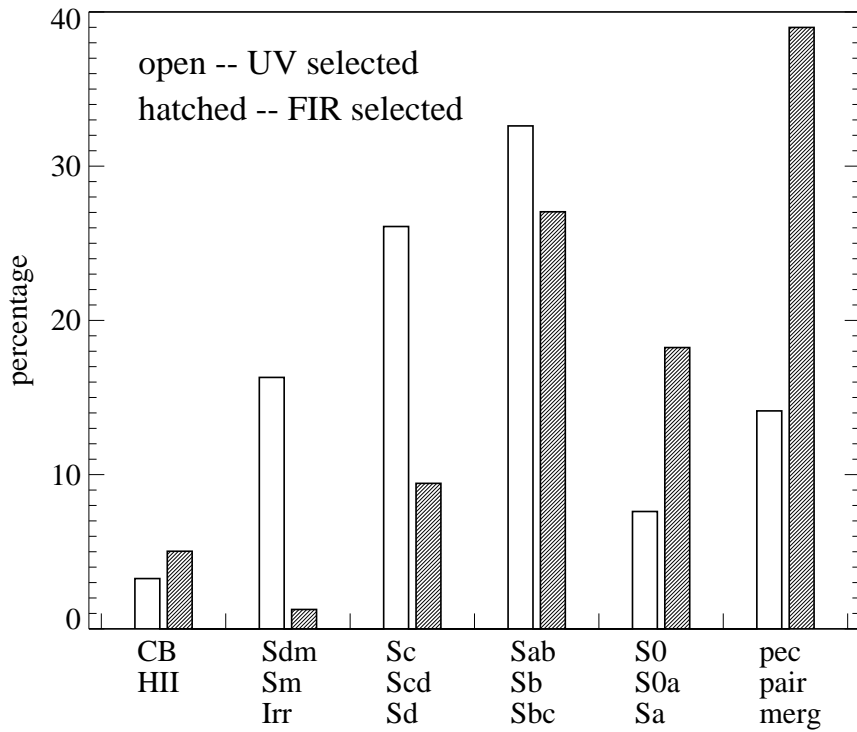


Figure 3: Morphological distributions of UV and IR galaxies.

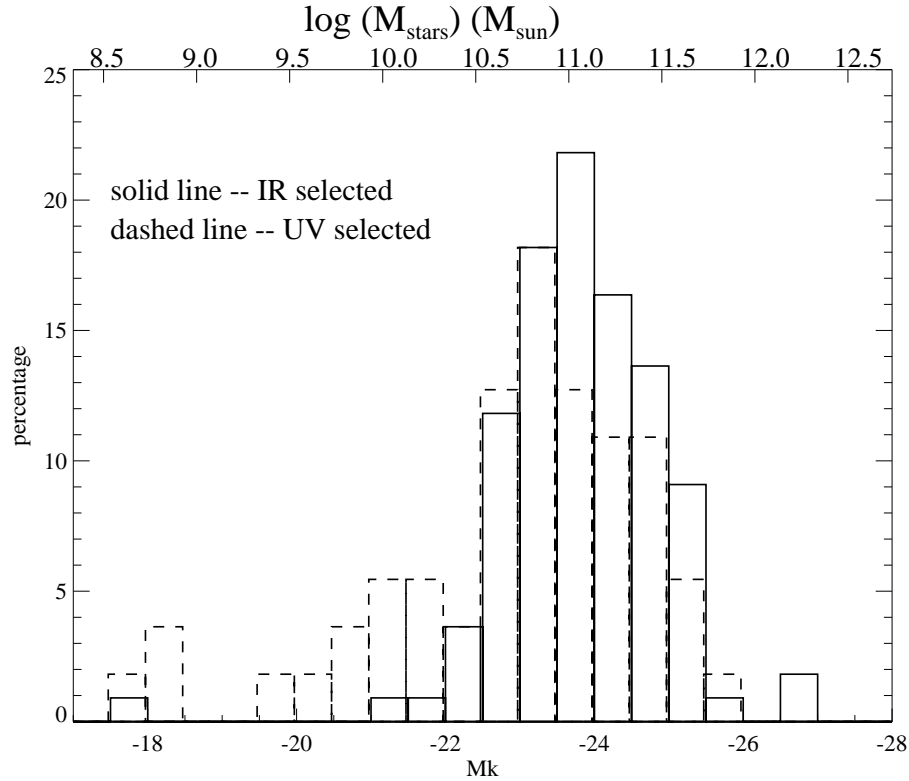


Figure 4: Stellar mass distributions of UV and FIR selected samples.

band absolute magnitude of the UV selected is  $-21.23$  and that of the IR selected sample  $-21.95$ . The conversion factor  $M_{\text{stars}}/L_{\text{K}} = 1.32M_{\odot}/L_{\odot}$ , which is derived for a stellar population with constant star formation rate and a Salpeter IMF<sup>17</sup>, is assumed when converting the K band luminosity to stellar mass. The median K band absolute magnitudes correspond to median stellar mass of  $10^{10.75} M_{\odot}$  for the UV selected sample and of  $10^{11.04} M_{\odot}$  for the FIR selected sample, respectively. Both medians are slightly lower than the mass corresponding to the K band  $L_{*}$  of 2MASS galaxies<sup>17</sup>. Here again there is a good overlap between the two populations, the medians differ only by less than a factor of 2. On the other hand, IR galaxies are slightly tilted for the more massive end, and more UV galaxies have relatively low mass.

The two plots in Fig.5 show that (1) UV galaxies which have the lowest mass also have the lowest  $L_{\text{tot}}$  and the lowest IR-to-UV ratio; (2) most massive IR galaxies are not the galaxies with the highest  $L_{\text{tot}}$ ; (3) the brightest galaxies have mass about  $M_{*}$ ; (4) for given mass, UV galaxies have lower  $L_{\text{tot}}$  and IR-to-UV ratio than IR galaxies.

In order to check how much UV and IR galaxies overlap and how much they miss each other, we have derived infrared luminosity function of UV galaxies, as plotted in Fig.6a by the open squares with error bars. It is compared it with the IRAS luminosity function shown by the solid line. The UV luminosity function of IR selected galaxies, as plotted in Fig.6b by the open diamonds with error bars, is compared to the GALEX luminosity function shown by the solid line. It appears that in the UV selected sample, galaxies of infrared luminosity larger than  $10^{11}$  solar luminosity are substantially under-represent (the ULIRGs being completely absent). In contrast, all UV galaxies brighter than  $10^9$  solar luminosity are fully represented in the IR selected sample, although some fainter UV galaxies could be missing in the IR sample.

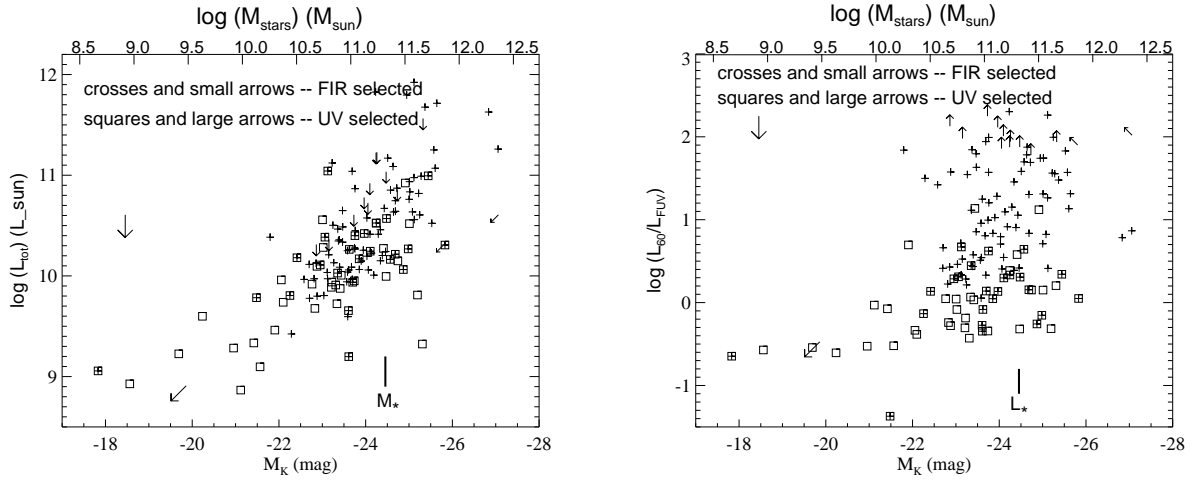


Figure 5:  $L_{tot}$  vs.  $M_{star}$  and FIR/UV vs.  $M_{star}$  of UV and IR galaxies.

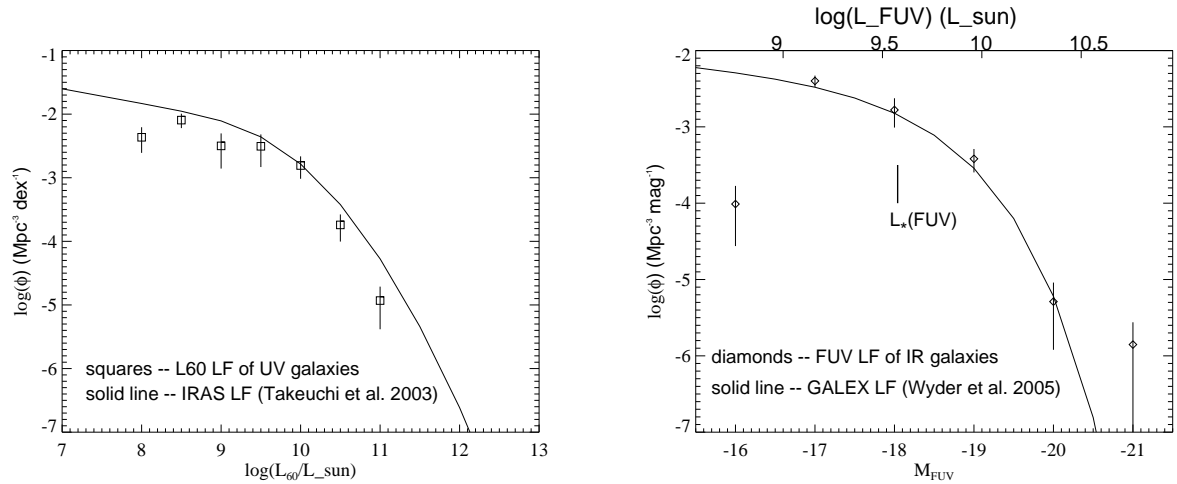


Figure 6: UV and IR luminosity functions. The GALEX FUV (1530Å) luminosity function is taken from Wyder et al. (2005), and the IRAS 60 $\mu m$  luminosity function is taken from Takeuchi et al. (2003).

### 3 Special Populations of UV Galaxies

The UV galaxies missed by IR surveys are so called ‘IR-quiet’ star-forming galaxies. The prototype is the famous low metallicity dwarf I-Zw-18. It has the lowest metallicity (1/50th of solar) known for galaxies, and its baryonic mass is only about  $2 \times 10^8 M_{\odot}$ . Its FUV luminosity as measured by GALEX is  $2.5 \times 10^8 L_{\odot}$ . I-Zw-18 has never been detected in far-infrared. The IRAS upperlimit corresponds to an upperlimit for the IR-to-UV ratio of less than 0.25.

Another prototype IR-quiet galaxy is SBS-0335-052. It has the second lowest known metallicity of 1/35th solar. The mass is higher than I Zw 18, about  $2 \times 10^9 M_{\odot}$ . It was undetected by IRAS, but detected by both ISO and Sptizer. Its IR SED reported by Houck et al.<sup>23</sup> is very different from that of ordinary galaxies: its  $f_{60\mu m}$  is about the same as  $f_{25\mu m}$  whereas normal galaxies such as the Milky Way has the  $f_{60\mu m}/f_{25\mu m}$  ratio  $\sim 5 - 10$ . In summary, IR quiet galaxies are dwarf galaxies of low metallicity, usually lower than 1/10th solar. They have relatively low mass and low UV luminosity. They are about 10 times fainter than the  $L_{*}$  of FUV, and about 100 times fainter than the Lyman Break Galaxies (LBG). Therefore they are no local counterparts of LBGs. Typically they have  $L_{60}/L_{UV} < 0.3$ . And they are less than 15% of galaxies in a UV selected sample.

The true local counterparts of Lyman break galaxies are a population of UV luminous galaxies, or UVLGs, recently discovered by GALEX<sup>20</sup>. These galaxies are brighter than  $L_{FUV} = 2 \times 10^{10} L_{\odot}$ . And they have a density about 100 times lower than that of LBGs, at  $\sim 10^{-5} \text{ Mpc}^{-3}$ . These galaxies can be divided into compact galaxies having higher surface brightness and lower mass, and the large galaxies having lower surface brightness and larger mass. The compact galaxies are similar to LBGs in terms of size and mass. Also, compact galaxies and LBGs have similar UV attenuation, star formation history parameter  $b$ , and the metallicity, while large galaxies have values in these variables differ from that of LBGs. Heckman et al.<sup>20</sup> identified compact UVLGs as the local counterparts of Lyman Breaks. In Fig.7, the UVLGs are compared with other population of UV and IR galaxies. By definition, UVLGs occupy the bright end of the UV population. But still, their  $L_{tot}$  does not go much beyond  $10^{11} L_{\odot}$ , never being as bright as ULIRGs. It appears that UVLGs have the dust attenuation in the same range as that of main population of UV selected galaxies. However, it should be pointed out that this result can be rather uncertain because, due to the lack of FIR data, the dust attenuation of UVLGs is estimated through SED fitting.

Lyman Break Galaxies (LBGs) and SCUBA galaxies are UVLGs and ULIRGs at  $z \sim 3$ . There is little overlap between these two populations. The SCUBA survey of LBGs by Chapman et al.<sup>14</sup> has only 1 detection. The works by Adelberger & Steidal<sup>1</sup> and Chapman et al.<sup>15</sup> show that nearly all LBGs have IR/UV ratio less than 100 while nearly all SCUBA galaxies have the ratio larger than 100. Compared to LBGs, SCUBA galaxies are heavier<sup>37</sup> and more strongly clustered<sup>6</sup>.

### 4 UV and IR Galaxies at $z = 0.6$ : GALEX/SWIRE Comparison

The first question is: why  $z=0.6$ ? There are several reasons for us to concentrate on this redshift. First of all,  $z=0.6$  is close to the peak of cosmic star formation suggested by the SDSS fossil studies of local galaxies<sup>22</sup>. Secondly, for larger redshift, the NUV band of GALEX is affected by the rest frame  $Ly_{\alpha}$  emission or absorption, therefore the K-corrections can be very uncertain. And finally, at  $z=0.6$ , there are several coincidences, which make the K corrections very straightforward: (1) the GALEX NUV band coincides with the rest frame FUV; (2) the MIPS  $24\mu m$  band measures the rest frame  $15\mu m$  emission, which is an infrared luminosity indicator extensively studied by ISO. And finally, the IRAC  $3.6\mu m$  band flux measures the rest frame K-band emission which is the best stellar mass indicator.

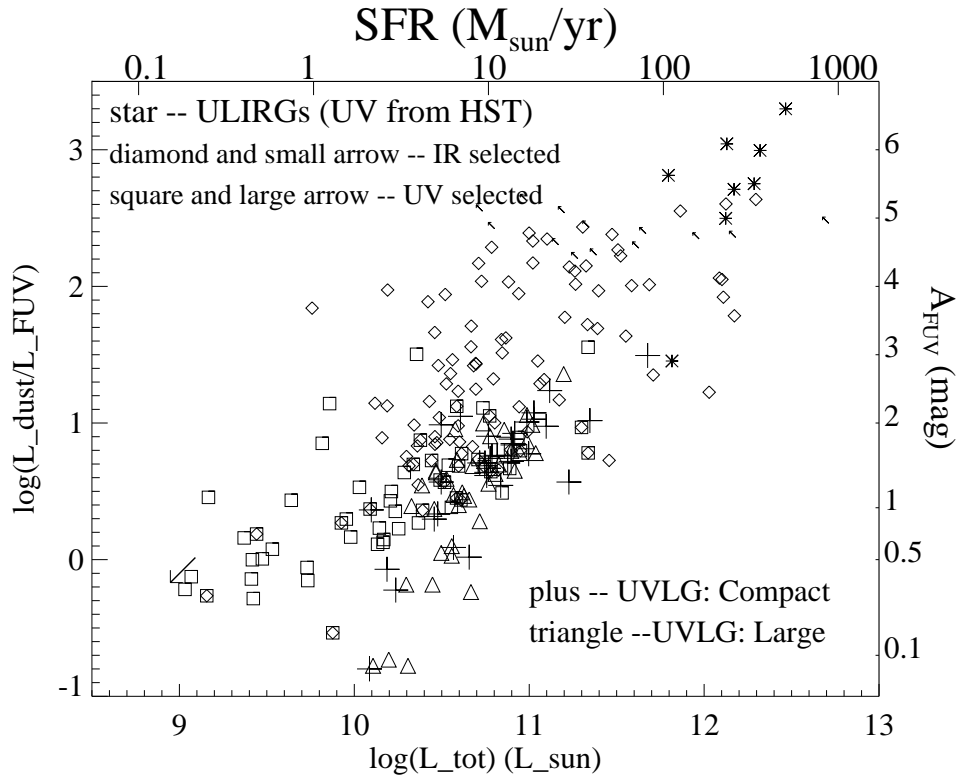


Figure 7: Comparison of UVLGs with other UV and IR populations. The data for UVLGs are taken from Heckman et al. (2005), and the data for ULIRGs are taken from Trentham et al. (1999) and Goldader et al. (2002).

The field studied is the GALEX ELAIS-N1.00 which is inside the SWIRE ELAIS N1 field, covering  $0.6 \text{ deg}^2$  of sky. The nominal  $5\sigma$  sensitivity limit of SWIRE  $24\mu\text{m}$  survey is  $f_{24} = 0.15 \text{ mJy}$ , but below  $f_{24} = 0.2 \text{ mJy}$  the catalog becomes progressively incomplete<sup>40 36</sup>. The GALEX NUV data are confusion limited at  $\text{NUV} \simeq 24$ . The photometric redshifts, derived using optical Ugriz magnitudes obtained in the ELAIS-N1 optical survey and SWIRE  $3.6 - 24\mu\text{m}$  flux densities, are taken from Rowan-Robinson et al.<sup>33</sup> which have rms deviation of  $\log_{10}(1+z)$  about 10%. In the area considered here, we select a sample of 1124 NUV sources which are brighter than  $\text{NUV}=24$  and which have the photometric redshifts in the range of  $0.5 \leq z \leq 0.7$ , and another sample of 316  $24\mu\text{m}$  sources brighter than  $f_{24} = 0.2 \text{ mJy}$  in the same photometric redshift range. Among the  $z \sim 0.6$   $24\mu\text{m}$  sources, 127(40%) are detected by GALEX in NUV, and the  $24\mu\text{m}$  detection rate of the  $z \sim 0.6$  NUV sources is only 14%. For GALEX sources not detected in  $24\mu\text{m}$  band, an upperlimit of  $f_{24} = 0.2 \text{ mJy}$  is assigned. For SWIRE sources not detected by GALEX, the NUV upperlimit corresponds to  $\text{NUV}=24 \text{ mag}$ . All galaxies in both samples are detected by SWIRE in the  $3.6\mu\text{m}$  band with the nominal sensitivity limit ( $5\sigma$ ) of  $f_{3.6} = 3.7 \mu\text{Jy}$ . The FUV luminosities ( $\nu L_{\nu}(1530\text{\AA})$ ) are derived from the NUV magnitudes and the photometric redshifts (hereafter photo- $z$ ). Given the large errors in photo- $z$ , the k-correction related uncertainties are neglected. In the same manner, we assume the Spitzer  $24\mu\text{m}$  observations measure the rest frame  $15\mu\text{m}$  emission in these galaxies, and the total dust luminosity is estimated using the conversion factor  $L_{dust} = 11.1 \times L_{15}$ <sup>16</sup>. The rest frame K band ( $2.2\mu\text{m}$ ) luminosities of these galaxies are calculated using the Spitzer  $3.6\mu\text{m}$  flux densities and the photo- $z$ . The stellar mass is estimated from the K-band luminosity using the mass-to-light ratio  $M_{\text{stars}}/L_{\text{K}} = 1.32 M_{\odot}/L_{\odot}$ <sup>17</sup>.

Because the  $f_{24}$  detection rate of the  $z=0.6$  UV sources is only 14%, the only way we can get meaningful information about the IR emission of these UV galaxies is through stacking. We

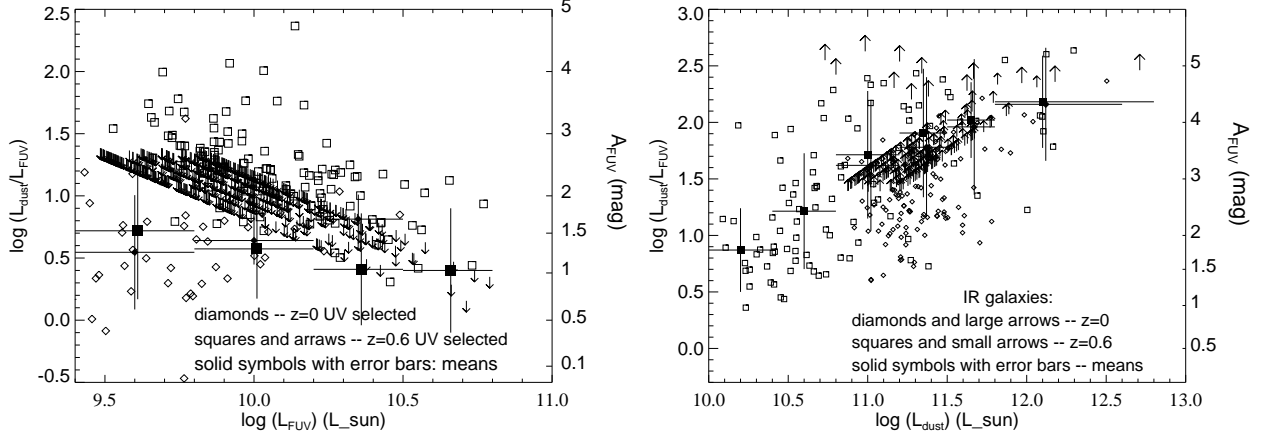


Figure 8:  $L_{dust}/L_{FUV}$  vs. luminosity plots of UV and IR galaxies: comparisons between galaxies at  $z=0.6$  and at  $z=0$ .

binned the UV galaxies into these 4 luminosity bins. Stacking the images of galaxies in each bins, we derived mean  $f_{24}$  and the mean  $L_{dust}/L_{FUV}$ . The latter are compared with the values of  $z=0$  galaxies in Fig.8a. There is no significant difference between the mean  $L_{dust}/L_{FUV}$  ratios of  $z=0$  and  $z=0.6$  galaxies, suggesting no evolution for the internal extinction in UV galaxies of the same luminosity. Indeed, for both samples, the mean  $L_{dust}/L_{FUV}$  ratios do not show significant dependence on the UV luminosity.

The NUV detection rate of  $24\mu m$  selected galaxies is 40%. We use both stacking method and the survival technique<sup>18 35</sup> to derive the means of  $L_{dust}/L_{FUV}$  of these galaxies in different  $L_{dust}$  bins, the results are plotted in Fig.8b. In contrast with the UV galaxies, both  $z=0.6$  and  $z=0$  IR galaxies show strong dependence of the  $L_{dust}/L_{FUV}$  with the luminosity. Indeed, IR galaxies in the luminosity range covered by the  $z = 0.6$  sample have significantly higher  $L_{dust}/L_{FUV}$  ratios than those of the UV galaxies (Fig.8a). On the other hand, as shown by the mean ratios, the IR galaxies of  $z=0.6$  have about the same  $L_{dust}/L_{FUV}$  as their  $z=0$  counterparts of the same IR luminosity.

The most serious uncertainty in the comparisons above is due to the extrapolation from  $L_{15\mu m}$  to  $L_{dust}$ . The most direct way to constrain this uncertainty is to look at the real SEDs of the  $z=0.6$  galaxies, in particular those detected in Spitzer MIPS  $70\mu m$  (rest frame  $43.75\mu m$ ) and  $160\mu m$  (rest frame  $100\mu m$ ) bands. In the sky region studied here, there is only one  $z \sim 0.6$  galaxy detected in  $160\mu m$  band. This source has an SED very close to that of Arp220, which has an  $L_{dust}/L_{15\mu m}$  about 3 times higher of that of Chary & Elbaz value. Among the other 4  $z \sim 0.6$  galaxies detected in the  $70\mu m$  band, two have SEDs similar to that of Mrk231 which has an  $L_{dust}/L_{15\mu m}$  about half of that of Chary & Elbaz value, other two have Arp220 type SEDs. These results indicate that the uncertainty due to variation of  $L_{dust}/L_{15\mu m}$  is about a factor of 2.

In Fig.9a we compare the stellar mass of  $z=0.6$  UV galaxies of given UV luminosity to their local counterparts. The stellar mass is estimated using the rest frame K band luminosity. The solid diamonds are the mean of the  $z=0.6$  galaxies, and the solid squares are the means of the local UV galaxies. Except for the last bin, in all other bins the stellar mass of  $z=0.6$  UV galaxies is about a factor of 2 less than that of the local UV galaxies. This is equivalent to a 2 times higher specific star formation rate in a given FUV luminosity. The comparison of the stellar mass of  $z=0.6$  and  $z=0$  IR selected galaxies is plotted in Fig.9b. Different from UV galaxies, there is no evidence for any evolution in the stellar mass of IR selected galaxies.

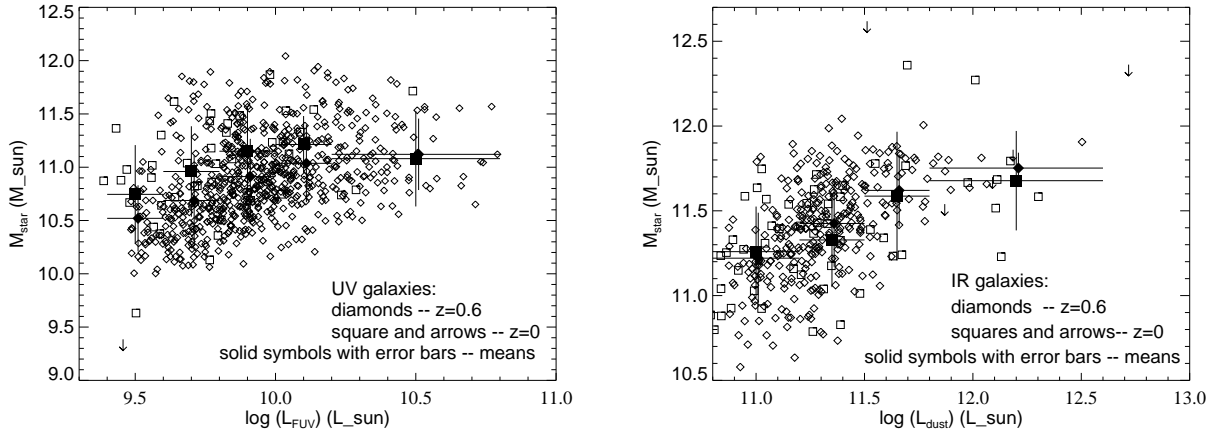


Figure 9: Stellar mass vs. luminosity plots of UV and IR galaxies: comparisons between galaxies at  $z=0.6$  and at  $z=0$ .

## 5 Summary

By selection, UV and IR galaxies have very different characteristic IR/UV ratios. The morphological and stellar mass distributions of UV and IR galaxies have good overlaps. IR galaxies brighter than  $L_{60\mu m} = 10^{11} L_{\odot}$  are severely under-represented in the UV sample, and a population of low mass, low luminosity UV galaxies are largely missing in the IR sample. In the local universe, the contribution from bright IR galaxies (LIRGs and ULIRGs) and from the ‘IR-quiet’ UV galaxies to the total star formation are negligible, the selection effect in the UV and IR samples does not introduce significant bias.

Star forming galaxies at intermediate redshifts ( $z \sim 0.6$ ) do not show significant evolution in the dust attenuation compared to their  $z=0$  counterparts of same luminosity. The strong evolution for the dust attenuation derived from the ratios of mean UV and IR luminosity density at different redshifts<sup>8</sup> is therefore due to the strong luminosity evolution of star forming galaxies and the dependence of the dust attenuation on  $L_{tot}$ . There is evidence for decrease of stellar mass of UV galaxies with redshift, indicating a continuous assembly of these galaxies in the recent history of the universe. No such evidence for the IR galaxies.

## Acknowledgments

Collaborations with Michael Rowan-Robinson, Jorge Iglesias-Páramo, Tsutomu T. Takeuchi, and other members of GALEX team and SWIRE team are acknowledged.

## References

1. Adelberger, K.L., Steidel, C.C. 2000, ApJ, 544, 218.
2. Bell, E. 2002, ApJ, 577, 150.
3. Bell, E. 2003, ApJ, 586, 794.
4. Bell, E., De Jong, R.S. 2001, ApJ, 550, 212.
5. Bell, E.F., McIntosh, D.H., Katz, N., Weinberg, M.D., 2003, ApJS, 149, 289.
6. Blain, A.W., Chapman, S.C., Smail, I., Ivison, R. 2004, ApJ, 611, 725.
7. Boselli, A., Gavazzi, G., Donas, J., Scodreggio, M. 2001, AJ, 121, 753.
8. Buat, V. 2004, in *The Spectral Energy Distribution of Gas Rich Galaxies*; eds. M. Dopita, C. Popescu, R. Tuffs; in press.
9. Buat, V., Burgarella, D. 1998, A&A, 334, 772.

10. Buat, V., Donas, J., Milliard, B., Xu, C. *A&A*, 352, 371.
11. Buat, V., Xu, C. 1996, *A&A*, 306, 61.
12. Buat, V., et al. 2005, *ApJL*, 619, 51.
13. Calzetti, D. 1997, *AJ*, 113, 162.
14. Chapman, S.C., et al. 2000, *MNRAS*, 319, 318.
15. Chapman, S.C., et al. 2004, *ApJ*, 2004, 614.
16. Chary, R., Elbaz, D. 2001, *ApJ*, 556, 562.
17. Cole, S., Norberg, P., Baugh, C.M., et al. 2001, *MNRAS*, 326, 255.
18. Feigelson, E.D., Nelson, P.I. 1985, *ApJ*, 293, 192.
19. Goldader, J.D., Meurer, G., Heckman, T.M., Seibert, M., et al. 2002, *ApJ*, 568, 651.
20. Heckmann, T.M., et al., 2005, *ApJL*, 619, 35.
21. Heinis, S., Treyer, M., Arnouts, S., Milliard, B., et al. 2004, *A&A*, 424, L9.
22. Heavens, A., Benjamin, P., Jimenez, R. Dunlop, J. 2004, *Nature*, 428, 625.
23. Houck, J.R., Charmandaris, V., Brandl, B.R., Weedman, D. et al. 2004, *ApJS*, 154, 211.
24. Iglesias-Páramo, J. Buat, V., Donas, J., Boselli, A., Milliard, B. 2004, *A&A*, 419, 109.
25. Iglesias-Páramo, J. 2005, this volume.
26. Iglesias-Páramo, J. et al. 2005, preprint.
27. Kauffmann, G., Heckman, T.M., White, D.M., Charlot, S., et al. 2003, 2003, *MNRAS*, 341, 33.
28. Kaplan, E.L., Meier, P. 1958, *J. Am. Statistical Assoc.*, 53, 457.
29. Kennicutt, R.C. 1998, *ARA&A*, 36, 189.
30. Kong, X., Charlot, S., Brinchmann, J. Fall, S.M. 2004, *MNRAS*, 349, 769.
31. Martin, D.C., et al., 2005, *ApJL*, 619, 59.
32. Meurer, G.R., Heckman, T.M., Calzetti, D. 1999, *ApJ*, 521, 64.
33. Rowan-Robinson, M., Babbedge, T., Surace, J., Shupe, D., et al. 2005, *AJ*, 129, 1183.
34. Saunders, W., Sutherland, W.J., Maddox, S.J., et al. 2000, *MNRAS*, 317, 558.
35. Schmitt, J.H.M.M. 1985, *ApJ*, 193, 298.
36. Shupe, D., et al., preprint.
37. Smail, I., Chapman, S.C., Blain, A.W., Ivison, R.J., *ApJ*, 616, 71.
38. Smail, I., Blain, A.W., Kneib, J.P. in *Deep millimeter surveys: implications for galaxy and evolution*, Proceeding of the UMASS/INAOE conference, Eds. J.D. Lowenthal & D.H. Hughes, 207p (Singapore: World Science Publishing).
39. Strauss, M.A., Davis, M., Yahil, A., Huchra, J.P. 1992, *ApJ*, 385, 421.
40. Surace, J. et al. 2004, *Cat.*, 2255, "SWIRE ELAIS N1 Source Catalogs".
41. Takeuchi, T.T., Yoshikawa, K., Ishii, T.T. 2003, *ApJL*, 587, 89.
42. Trentham, N., Kormendy, J. K., Sanders, D. B. 1999, *AJ*, 117, 2152.
43. Wang, B., Heckman, T.M., 1996, *ApJ*, 457, 645.
44. Wyder, T., et al. 2005, *ApJL*, 619, 15.
45. Xu, C., Buat, V. 1995, *A&A*, 293, L65.